What can calorimetry tell us about changes of three-dimensional aggregate structures of phospho- and glycolipids?

K. Brandenburg[a,*], P. Garidel[b], J. Howe[a], J. Andrä[a], L. Hawkins[c], M.H.J. Koch[d], U. Seydel[a]

[a]Forschungszentrum Borstel, Parkallee 10, D-23845 Borstel, Germany
E-mails: jhowe@fz-borstel.de, jandrae@fz-borstel.de, useydel@fz-borstel.de

[b] Martin-Luther-Universität Halle/Wittenberg, Mühlpforte 1, D- 06108 Halle.
E-mail: patrick.garidel@t-online.de

[c]Eisai Research Institute, 4 Corporate Drive, Andover, MA, USA.
E-mail: lynn_hawkins@eri.eisai.com

[d]European Molecular Biology Laboratory c/o DESY, Notkestr. 52, D-22603 Hamburg, Germany
E-mail: Koch@embl-hamburg.de

*Corresponding author:

Address: Forschungszentrum Borstel, Leibniz-Zentrum für Medizin und Biowissenschaften

Parkallee 10, D-23845 Borstel, Germany.
E-mail: Kbranden@fz-borstel.de
Tel:+49(0)4537-188235
Fax: +49(0)4537-188632

Abstract

It is reported on the structural polymorphism of the main amphiphilic cell membrane compounds, phospholipids and glycolipids, with special regard to calorimetric analyses. These lipids may form a large variety of aggregate structures in dependence on their chemical primary structure, on temperature, water content, and concentrations of cations. The entity of aggregate structures is usually called the phase diagram of the respective lipids. This should, however, not to be confused with the gel and liquid crystalline phases of the hydrocarbon chains of lipids, which differ in the fluidity of the acyl chains, and between which a first order transition can be observed. Thus, in this contribution exemplary results are presented on the structural behaviour of biologically important lipids including their phase behaviour and structural preferences under different ambient conditions, and how phase and structural transitions are connected with enthalpic changes.

Keywords: Structural polymorphism, phase transition, phase diagram, phospholipids, glycolipids

Abbreviations: DSC differential scanning calorimetry, LPS lipopolysaccharide(s), FTIR Fourier-transform infrared spectroscopy

1. Introduction

Procaryotic as well as eucaryotic cells are surrounded by a cell envelope which is, in the simplest case, one cell membrane, and in more complex cases comprise further membranes or layers, which separates the cytoplasm from the aqueous extracellular space. Cell membranes are composed of a double layer made from phospholipids (Fig. 1, [1]). Within this double layer various peripheral and integral proteins, cholesterol and glycolipids and -proteins, the latter having a covalently-linked short or long sugar chain on the outside, are incorporated [2]. The main function of the lipid matrix is that of a barrier for hydrophilic compounds and ions, and the additional structures are responsible for other important functions such as cell nutrition and communication of the cell with its surrounding, i.e., maintain a dynamic equilibrium within the cell. For example, glycolipids and glycoproteins (glycoconjugates) may act as cell receptors, provide specific contact, be important for cell adhesion and aggregation, and be responsible for cell signalling [3]. Furthermore, in the case of bacteria their membranes are the primary target of the attack of the defence system of animals and humans as well as of antibiotics.

Many of these molecules are not in the homogenous membrane ‘bulk’, but are present in particular domains such as lipid rafts [4,5], in which also the lipid pattern can be assumed to be changed as compared to the ‘bulk’ lipid. Moreover, for most cells permanent anabolic and catabolic processes (build-up and decomposition) take place. To these belong the transport of lipids into/out of the cells, and the transport through the humoral system, for example phospholipid transfer by proteins such as HDL (high-density lipoprotein). Finally, lipid polymorphism today is also of high relevance with respect to technological applications, for example in drug delivery research using phospholipid liposomes [6,7].

Thus, from all these reasons an understanding of the structural behaviour of the cell membrane constituents is of uttermost interest. In this contribution an overview of the physicochemical properties of these compounds as well as selected examples for phospho- and glycolipids are given. It should be noted that there is an overwhelming number of calorimetric studies on membrane lipids. Therefore, here only a more or less arbitrary section of these papers can be presented.

2. Materials and methods

Lipids and reagents

The phospholipids dipalmitoyl phosphatidylcholine (DPPC), dimyristoyl phosphatidylglycerol (DMPG), and 1-palmitoyl-2-oleoyl-phosphatidylethanolamine (POPE) were purchased from Avanti Polar Lipids (Alabaster, Al, USA).

Lipopolysaccharide (LPS) from the rough mutant Ra *Salmonella minnesota* strain R60 was extracted by the phenol/chloroform/petrol ether method [8] from bacteria grown at 37°C, purified, and lyophilised. Lipid A was isolated from LPS by mild acid hydrolysis using acetate buffer (pH 4.4) treatment (0.1 M, 100 °C for 2 h, [9]), purified, and subsequently converted into the triethylammonium salt form.

The phospholipid-like structure ER803022 was synthesized at Eisai Research Institute of Boston, Andover, MA as described recently [10]. The peptide polymyxin B (PMB) was purchased from Sigma (Deisenhofen, Germany). The antimicriobial peptide NK-2 consists of the 27-amino acid residue cationic core region of mammalian antibacterial effector protein NK-lysin [11].

Sample preparation

The lipid samples were usually prepared as aqueous dispersions (1 to 10 mM) for the phase transition measurements (DSC, FTIR). For X-ray diffraction experiments, a 50 mM dispersion was prepared. The lipids were prepared by suspending them directly in 20 mM HEPES buffer, pH 7.0, sonicating and temperature-cycling for several times between 5 and 70 °C and then storing at 4 °C for at least 12 h before measurement.

Differential Scanning Calorimetry (DSC)

A stock solution of 1 mg/ml of the phospholipids, LPS Ra or lipid A was dispersed in an appropriate buffer solution (see text). Lipid aggregates were obtained by sonication as described previously [12, 13]. Differential scanning calorimetry (DSC) measurements were performed with a MicroCal VP scanning calorimeter (MicroCal, Inc., Northhampton, MA, USA) at heating and cooling rates of 1° C/min. Heating and cooling curves were measured in the temperature interval from 10 to 95 °C. Three consecutive heating and cooling scans were measured. For more details see Blume and Garidel [14].

FTIR spectroscopy

The infrared spectroscopic measurements were performed on a IFS-55 spectrometer (Bruker, Karlsruhe, Germany). For the phase transition measurements via the analysis of the peak

position of the symmetric stretching vibrational band $\nu_s(CH_2)$ of the methylene groups around 2850 cm^{-1}, the lipid samples were placed in a CaF_2 cuvette with a 12.5 µm teflon spacer. Temperature-scans were performed automatically between 10 and 70 °C with a heating-rate of 0.6 °C/min. Every 3 °C, 50 interferograms were accumulated, apodized, Fourier transformed, and converted to absorbance spectra.

X-ray diffraction

X-ray diffraction experiments to define aggregate structures of the endotoxins were performed at the European Molecular Biology Laboratory (EMBL) outstation at the Hamburg synchrotron radiation facility HASYLAB using the double-focussing monochromator-mirror camera X33 [15]. X-ray diffraction patterns, obtained with exposure times of 2 min using a linear gas proportional detector with delay line readout [16] were evaluated according to previously described procedures [17]. These allow to assign the spacing ratios to defined three-dimensional aggregate structures, from which the conformation of the individual molecules are deduced.

3. Results and Discussion

General remarks

The most prominent calorimetric methods in biophysical lipid research are differential scanning calorimetry (DSC) and isothermal titration calorimetry (ITC). The latter method, in which at a constant temperature heat effects due to the interaction of two reaction partners are measured, will not be considered here. For more details see [14].

The basic principles of the structural polymorphism of lipids, which includes the preference for particular aggregate structures, and of the gel to liquid crystalline ($\beta \leftrightarrow \alpha$) phase behaviour, both in dependence on temperature, water content, and cation concentrations, were described earlier [18-20]. Briefly, above the lipid-specific critical micellar concentration (CMC, sometimes also called critical aggregate concentration CAC) the lipids form stable aggregates. Depending on the chemical structures of the respective lipids, various molecular shapes can be observed which may lead to a variety of possible supramolecular three-dimensional structures (Fig. 2). These structures may be grouped according to the ratios of the molecular cross-sections of the hydrophilic to the hydrophobic moieties, which may be expressed by a dimensionless shape parameter $S = v/(a_0 \cong l_c) = a_h/a_0$, v = volume of the hydrophobic moiety,

a_0 and a_h = cross-sectional areas of the hydrophilic and hydrophobic moieties, respectively, l_c = length of the fully extended acyl chains [21]. For small values of S, micellar (true micelles, not to mix with the term 'micelles' as synonym for aggregates, see above), H_I or cubic Q_I (I means acyl chains inside, headgroups outside) are adopted. For S-values around 1, various lamellar (L) structures are formed, e.g., flexible bilayers (uni- or multilamellar) as vesicles (liposomes) or planar bilayers (also uni- or multilamellar). For S>1, the preferred three-dimensional structures are of cubic symmetry, Q_{II}, or inverted hexagonal, H_{II} (II means acyl chains outside, headgroups inside). Phases with ondulated rather than plane surfaces are called P-phases.

Within the aggregate structures, the hydrocarbon chains may assume two basic states, the gel phase (β), in which the chains are in the zig-zag configuration (*all-trans*) and the liquid crystalline phase (α), in which the chains become more and more disordered due to the introduction of *gauche* conformers ([22], Fig. 3). Between these two phases a reversible first order transition at a temperature T_m or T_c ('main' or 'critical' transition) takes place, the value of which depends again on the chemical structure of the (glyco)lipid and the environmental conditions place. It should be noted that both phases can not necessarily be observed in each structure presented in Fig. 2. In the case of highly curved surfaces such as found in spherical and cylindrical micelles and within the H_{II} structure, only the liquid crystalline phase is observed. This is connected with the fact that gel phase lipids are not able to form a lipid alignment of sufficiently high mobility and flexibility.

Pioneering investigations into the structural polymorphism of membrane lipids, in particular with calorimetric methods, have been published by the groups of Chapman and Sturtevant (see, for example [23-26]). Data from these papers, however, will not be presented here. Furthermore, Koynova and Caffrey [27] have published on overview on phases and phase transitions of phosphatidylcholines (lecithins). A summary of these quantities for various lipids is given by the Internet data bank Lipidat.

Acyl chain melting transitions

The gel to liquid crystalline $\beta \leftrightarrow \alpha$ acyl chain melting transition can be easily monitored via DSC by preparing phospholipid liposomes (Fig. 4) for example by sonication to give small unilamellar vesicles (SUV's, [28]). In this way, a very sharp calorimetric transition at T_m is observed, for example for zwitterionic dipalmitoyl phosphatidylcholine (DPPC, Fig. 5) at 41.5 °C [29]. However, the occurrence of a further small endotherm around 36 °C indicates a more complex behaviour than that of a simple $L_\beta \leftrightarrow L_\alpha$ transition. This 'pretransition' is indicative

of a transition from a tilted gel phase ($L_{\beta'}$) into an ondulated gel phase ($P_{\beta'}$), in which the bilayer surface displays a periodic ripple structure, while the main transition with ΔH_{cal} = 35 kJ/mol represents the acyl chain melting. For phosphatidylcholines an additional phase transition at low temperature is observed, when the hydrated $L_{\beta'}$ phase is dehydrated leading to a crystalline-like lamellar L_c phase. This $L_c \leftrightarrow L_{\beta'}$ phase transition shows a large hysteresis and is kinetically hindered (data not shown) [30].

At the temperature maximum T_m of the heat capacity curve, the degree of transition Θ describing the transition from phase A to phase B is $\Theta = 0.5$. Integration of the heat capacity curve yields the phase transition enthalpy ΔH_{cal}. For cooperative transitions like the lipid phase transition where intermolecular cooperativity is involved, the calorimetrically determined phase transition enthalpy ΔH_{cal} is much lower than the van't Hoff enthalpy ΔH_{vH}. Based on these values, the cooperative unit size n, which is a measure for the degree of cooperativity (same state of order) between the lipid molecules, can be calculated as: $n = \Delta H_{vH} / \Delta H_{cal}$. It is found that n is much larger than unity [31]. For the case of a true first-order phase transition this ratio approaches infinity and for the case of a completely non-cooperative equilibrium this ratio is unity. The van't Hoff enthalpy ΔH_{vH} can be calculated as: van't Hoff enthalpy $\Delta H_{vH} = 4 \cdot R \cdot T^2_m (d\Theta / dT)$, with R the gas constant, T the temperature. The van't Hoff enthalpy can also be estimated directly from the half height width $\Delta T_{1/2}$ of the heat capacity curve according to Mabrey and Sturtevant [31]: ΔH_{vH} (cal/mol) $\cong 6.9 \cdot T^2_m / \Delta T_{1/2}$ (as can be seen, this approximation is a pure numeric equation, the unit for T is K).

The accuracy of this expression is 10% of the real value. From ΔH_{cal} and T_m the transition entropy $\Delta S = \Delta H_{cal} / T_m$ can be calculated due to the fact that the Gibbs energy $\Delta G = 0$ at T_m.

Using this approach for the calculation of ΔS, it was found for phospholipids for an additional CH_2 unit in the acyl chains, that the entropy change is much lower as observed for the melting of pure hydrocarbons or long-chain fatty acids. This is an indication for a relative high degree of order in the liquid crystalline state of phospholipid bilayers and that the liquid crystalline phase is drastically different compared to an isotropic solution. The amount of bound versus free water in lipids can also be derived from calorimetric measurements (for more details see Blume [20]).

Furthermore, Blume [32,33] has shown, that DSC can also be used to determine the heat capacity of the dispersed lipid itself. A prerequisite for this type of measurement is a calorimeter instrument with a highly reproducible and stable base line. The apparent molar

heat capacity ^{Ø}Cp of a dispersed lipid can be calculated according to a procedure described by Privalov and Khechinashvili [34]:

$$^{Ø}Cp = [Cp_w (V_L / V_W) – \Delta / m_L] M_L,$$

with M_L the molecular weight of the lipid, m_L the mass of the lipid in the sample cell, V_L and V_W the specific volume of the lipid and water, respectively, Cp_w the specific heat of water, and Δ the displacement of the base line (in cal/K) in a DSC run with the sample in the cell compared to the base line recorded with buffer in both cells. The absolute values of ^{Ø}Cp contain important information on lipid-water interactions (e.g. hydrophobic hydration) (for more details see [33]). This parameter give a more comprehensive insight in the organisation and structure of lipid bilayers.

As further example of DSC heating curves, the results for the negatively charged dimyristoyl phosphatidylglycerol (DMPG) are presented in Fig. 6. The sample was not heated but rather kept at 4 °C for several days prior to measurement, and showed in the electron micrograph a 'cochleate' phase [35]. The acyl chain melting of this phase led in the first scan (1^{st} h.s.) to a sharp transition at 40 °C into the L_α phase, while in the subsequent cooling scan (1^{st} c.s.) an exotherm around 23 °C was found. In the second heating scan, the 'normal' phase behaviour of DMPG is exhibited with an $L_{\beta'} \leftrightarrow P_{\beta'}$ pretransition (β' indicates tilted chains) around 15 °C and the main $P_{\beta'} \leftrightarrow L_\alpha$ main transition around 25 °C. The exact structure of the different phases was determined by synchrotron radiation X-ray small-angle scattering [35].

The interaction of cations, in particular divalent cations such as Mg^{2+} and Ca^{2+}, with negatively charged lipids is of particular physiological relevance. The different roles of Mg^{2+} and Ca^{2+} become apparent in the DSC scans presented in Fig. 7. Increasing amounts of Mg^{2+} lead – beside the main transition at 25 °C – to a further endotherm around 60 to 70 °C, which can be attributed to a dehydration process in lipid domains complexed with Mg^{2+} (Fig. 7A,C [35]). For more details see Garidel and Blume [36]. In further heating-scans, however, this transition disappears completely (as shown for the 3^{rd} heating-scan). For Ca^{2+} (Fig. 7B,D), the induction of this second endothermic peak takes place at significantly higher temperatures (80 to 90 °C), and, in contrast to Mg^{2+}, this dehydration process still takes place also in further scans [37, 38].

For the DMPG-Ca^{2+} systems it could be shown that between 50 and 80 °C a thermodynamically stable phase is formed. Below 35 °C, however, a metastable phase seems to exist, unless the sample is stored for several days at low temperature [36]. Thus, DSC can be used to identify the formation of metastable phases.

Interesting DSC-studies with respect to the behaviour of complex lipid mixtures have been published by Masserini et al [39,40]. These authors were interested in the analysis of lipid domains consisting, for example, from sphingomyelin, ganglioside, and cholesterol. Such investigations are important with respect to the biological importance of lipid domains like 'rafts', in which many cellular processes, e.g. adhesion, recognition, and cell signalling are assumed to take place [41]. Their DSC data indicate that in the mixed lipids lateral phase separation takes place, and that more ordered, higher melting ganglioside-enriched domains are present within a sphingomyelin bilayer [39]. The authors deduced this from the analysis of the DSC curve by a curve-fitting procedure thus resolving the respective contribution of the single components. In a similar way, they analysed the interaction of human glycophorin and glycosphingolipid embedded in DMPC vesicles [40].

As an example for the phase behaviour of a natural glycolipid, lipopolysaccharide (LPS, endotoxin) Ra from *Salmonella minnesota* strain R60 was monitored. LPS is an important glycolipid from the outer membrane of Gram-negative bacteria and is responsible for a variety of biological activities in mammals ranging from beneficial to pathophysiological ones such as the septic shock syndrome [42]. LPS consists of a lipid moiety called lipid A, and a covalently-linked oligo- or polysaccharide moiety, the length of which depends on the bacterial mutant (see mutant LPS from *Salmonella minnesota in* Fig. 8). Lipid A is responsible for its innate immune stimulating activity ('endotoxic principle'), and consists in enterobacteria mainly of a hexaacyl moiety with mostly myristoyl residues and two phosphate groups linked to a diglucosamine backbone. The gel to liquid crystalline acyl chain melting in Fig. 8 shows a very broad transition range of nearly 20 °C with a maximum around 36 °C, and a phase transition enthalpy ΔH_{cal} = 20 kJ/mol. The thermodynamic data for the cooling scan are: T_m = 35 °C with ΔH_{cal} of -11 kJ/mol. The broadness of the transition is characteristic for the heterogeneity of this natural compound, exhibiting non-stoichiometric substitutions of particular molecular groups within the lipid A moiety as well as in the sugar part. Furthermore, from the low ΔH = 20 kJ/mol for its hexaacyl lipid A part as compared to the 28 kJ/mol for corresponding saturated diacyl phospholipids (DMPC, DMPE [43]) it was interpreted that the packing density of the acyl chains is much lower than those of saturated phospholipids [44] (see, however, the discussion later).

DSC measurements are also very efficiently used for the construction of phase diagrams of e.g. a binary lipid system, in which a number of samples have to be analysed. Based on the analysis of the heat capacity curves using different thermodynamic models (e.g. regular solution theory), parameters describing the interaction between lipids can be derived and thus

the miscibility of lipids in a phase. This has been described recently by Garidel and co-workers [45, 46].

Changes of aggregate structures

Beside the ability of calorimetry to monitor the acyl chain melting transition, it should also allow to detect transitions between the different structures shown in Fig. 2. Of course, it cannot be excluded that an acyl chain melting is connected with a change of the aggregate structures.

The phospholipid 1-palmitoyl-2-oleoyl phosphatidylethanolamine (POPE) can serve as an example for an acyl chain melting transition and a transition between aggregate structures occurring in one and the same lipid at different temperatures. POPE performs an $L_\beta \leftrightarrow L_\alpha$ transition at 25 °C and an $L_\alpha \leftrightarrow H_{II}$ transition around 65 °C [47]. As can be seen from Fig. 9A, the former transition exhibits the usual sharpness and height, the second transition, however, is only very weak, although this transition corresponds to a considerable reorientation of the lipid aggregates. In a series of experiments, the action of the synthetic antimicrobial peptide NK-2 derived from the porcine defense protein NK-lysin on POPE as mimetic of bacterial phospholipids was studied. As apparent from Fig. 9B-D, increasing amounts of NK-2 lead to a decrease and broadening of the peak corresponding to the main transition, while there is a clear increase and sharpening of the peak corresponding to the transition into the H_{II} structure [11].

As further example for the structural behaviour of a lipid under different concentrations of a peptide the system lipid A and polymyxin B (PMB) is presented. Lipid A exhibits a main phase transition around 43 °C with ΔH_{cal} = 43 kJ/mol, which, however, takes place within a cubic structure or a mixed cubic/unilamellar structure [17]. The addition of PMB leads to a change of the aggregate structure into a multilamellar one [48]. The DSC scans (Fig. 10A) clearly show that the main acyl chain melting transition weakens in the presence of PMB eventually disappearing at the highest PMB concentrations. A strong decrease of the phase transition enthalpy is observed with increasing amount of peptide, whereas the maximum of the heat capacity curve is more or less unchanged and located between 42 – 43 °C.

Essentially two interpretations of this disappearance are plausible: (i) the acyl chain moiety of lipid A remains in the gel phase at all temperatures or (ii) is *a priori* in a highly fluid state already at low temperatures. To differentiate between these two possibilities Fourier-transform infrared spectroscopy (FTIR) was used, utilizing the fact that the peak position of

the symmetric stretching vibration around 2850 cm^{-1} is a measure of lipid order [49]. As can be seen in Fig. 10B, the addition of PMB to lipid A increases the wavenumber values at low temperatures, according to a massive fluidization in the gel phase [48]. Thus, the first interpretation mentioned above holds true, the acyl chains are completely in the fluid phase already at 10 °C due to peptide binding.

DSC scans of the phospholipid-like compound ER803022, a hexaacyl compound with a serine-like backbone and two phosphates, are shown as last example for the aggregation behaviour of lipids (Fig. 11A). This compound exhibits a $\beta \leftrightarrow \alpha$ phase behaviour around 10 °C and adopts a cubic aggregate structure up to 60 °C [50,51]. As can be seen in Fig. 11, in the first heating-scan only a small ΔH = +8 kJ/mol is observed at the phase transition, which, however, increases to approximately +16 kJ/mol in the following scans. The phase transition enthalpy for the re-crystallisation from the liquid crystalline phase to the gel phase is about –8 kJ/mol. Further experiments were performed with the same compound in the presence of an equimolar content of Mg^{2+} (Fig. 11B). The DSC scans are indicative of two structural transitions around 22 (ΔH_{cal} = +4 kJ/mol) and 40 °C (ΔH_{cal} = +7 kJ/mol). The phase transition enthalpies for the cooling scans are in the average ΔH_{cal} = -4 (21.5 °C) and -7 kJ/mol (37.4 °C).

Again FTIR was used to get closer insights into the type of the transitions in the absence and presence of Mg^{2+} (Fig. 11B). Clearly, the acyl chain melting transition around 10 °C in the absence of Mg^{2+} (see Fig 11A, top) is shifted to a higher temperature (around 20 °C) and the transition is sharpened in accordance to the DSC data. Furthermore, there seems to be also a transition around 40 to 45 °C in the presence of Mg^{2+}, but not as pronounced as in the DSC experiment.

From findings with other negatively charged lipids it may be speculated that the first transition may be a transition within lamellar structures and the second one into a H_{II} structure. To verify this, synchrotron radiation small-angle X-ray diffraction was applied (Fig. 13). It can be clearly deduced from Fig. 13A that (i) the reflections occurring at equidistant ratios correspond to a multilamellar structure and that (ii) the jump of the periodicity between 20 and 30 °C from 4.57 to 4.35 nm indicates an $L_\beta \leftrightarrow L_\alpha$ transition. In Fig. 13b, it can be seen that the reflections at 35 °C are still typical for a multilamellar structure, but change completely at 50 °C into a pattern with the occurrence of a main reflection at 4.95 nm and two further reflections at $1/\sqrt{3}$ and $1/\sqrt{4}$ of the former , which is characteristic for a H_{II} structure.

Interesting are the enthalpy changes of the two transitions (Fig. 11B). Whereas for ‘normal’ phospho- and glycolipids the $L_\beta \leftrightarrow L_\alpha$ transition exhibits high and the $L_\alpha \leftrightarrow H_{II}$ low enthalpy

changes, the latter being only approximately 5 % of the former, this picture has completely changed: The transition into the inverted H_{II} structures now exhibits an enthalpic change larger than that of the acyl chain melting transition, which again is considerably less than that in the absence of Mg^{2+} (Fig. 11). The reason for this behaviour is not yet clear, but it may be assumed to be connected with exothermic reactions in the headgroup region during the transition, which reduce the endothermic acyl chain melting process. Such a process was addressed for lecithins in an earlier study by Mellier [52]. Generally, differences in headgroup hydration and changes upon chain melting might explain (i) differences between phospholipids and LPS with comparable chain lengths, (ii) the reduction of ΔH of compound ER803022 as compared to lipid A despite similar chemical composition of the hydrophobic moiety, and (iii) changes upon binding of divalent cations to negatively charged lipids. Details of these processes should be elucidated in further investigations

4. Conclusions

In the present paper, the suitability of DSC for monitoring structural changes in aqueous dispersions of lipids was demonstrated, which includes the detection of a pure acyl chain melting transition (‘phase transition’) as well as structural transitions between different three-dimensional structures. The most pronounced enthalpy changes are observed for the acyl chain melting either within a lamellar or non-lamellar supramolecular arrangement, whereas structural transitions, which are not accompanied by acyl chain melting, exhibit much lower enthalpy changes. Based on the analysis of the heat capacity curve and using appropriate thermodynamic models, further information concerning e.g. lipid-lipid interaction can be obtained. An important point is, that DSC is a rather fast method, requiring only low amounts of sample. The accuracy for the temperature determination is approx. ± 0.1 °C. It allows the investigation of changes of the phase transition as a function of an external perturbation (temperature, pressure or the presence of an interaction partner).

For an absolute determination of the respective aggregate structures, as method of choice X-ray diffraction, however, must be applied.

Acknowledgements

We thank B. Fölting for performing the DSC and G. von Busse the IR spectroscopic measurements. The study has been carried out with financial support from the Deutsche Forschungsgemeinschaft (SFB 470, project B5) and from the Commission of the European Communities, specific RTD programme 'Quality of Life and Management of Living Resources', QLCK2-CT-2002-01001, "Antimicrobial endotoxin neutralizing peptides to combat infectious diseases".

Figure Legends:

Fig. 1: General model of a cell membrane, consisting of a double layer of phospholipids, and integral and peripheral composites such as cholesterol, proteins, and glycoconjugates (glycolipids and –proteins), adapted from the original model of Singer and Nicholson [1].

Fig. 2: Molecular shape of amphiphilic lipids and the supramolecular shapes they may form, adapted from Israelachvili [21].

Fig. 3: States of order of acyl chains in *all-trans* (top) and mixed *trans-gauche* (bottom) conformations. On the righthand side, the Newman projections for these conformations are shown. Frequently, one *gauche* rotation by 120° is followed by another *gauche* rotation of –120° of either of the two next-nearest neighbouring bonds (= kink: gtg); adapted from Jain [22].

Fig. 4: Model of a flexible phospholipid bilayer ('liposome' or vesicle) typical for phosphatidylcholines (=lecithins). Sonification of the lipid results in the production of small unilamellar vesicles (SUVs) [7].

Fig. 5: Schematic DSC scan of dipalmitoylphosphatidylcholine (DPPC) indicating a pretransition at 36 °C, resulting from the transition from an inclined phase with rigid chains ($L_{\beta'}$) into an ondulated phase ($P_{\beta'}$) also with rigid chains, and a main phase transition at 41.5 °C, resulting from the transition of $P_{\beta'}$ into the liquid crystalline phase L_{α}.

Fig. 6: DSC scans of negatively charged dimyristoylphosphatdylglycerol (DMPG, concentration 1 mg/ml). Before the first scan, the lipid sample was cooled to 4 °C, exhibiting a 'cochleate' phase below T_m. In the following scans, the 'normal' phase behaviour $L_{\beta'} \leftrightarrow P_{\beta'} \leftrightarrow L_{\alpha}$ is observed.

Fig. 7: DSC scans of negatively charged DMPG (concentration 1 mg/ml) in the presence of varying concentrations of Mg^{2+} (A) and Ca^{2+} (B) of the first heating scan and for the third heating scan Mg^{2+} (C) and Ca^{2+} (D) (molar ratios). Beside the phase transitions observed for pure DMPG (see Fig. 6), a further phase around 60 to 70 °C (Mg^{2+}) and 80 to 90 °C (Ca^{2+}), respectively, is observed, which is connected with dehydration of DMPG (adapted from Garidel and Blume [36]).

Fig. 8: Schematic chemical structure and DSC scans of lipopolysaccharide (LPS) Ra from *Salmonella minnesota*, strain R60. In further cooling and heating scans the picture does not change. The broadness of the acyl chain melting transition is indicative of the heterogeneity of this natural product.

Fig. 9: DSC scans of 1-palmitoyl-2-oleoyl phosphatidylethanolamine (POPE) in the presence of different concentrations of the peptide NK-2. [POPE]:[NK-2] = 1:0 (A), 3000:1 (B), 300:1 (C), and 30:1 molar (D). Adapted from Willumeit et al [11].

Fig. 10: DSC scans (A) and temperature dependence of the peak position of the symmetric stretching vibration of the methylene groups (FTIR measurement, B) of lipid A from LPS Re *Salmonella minnesota* strain R595 in the presence of different concentrations of polmyxin B (PMB) (in molar ratios). The FTIR data were adapted from Brandenburg et al. [48].

Fig. 11: DSC scans of the hexaacyl phospholipid-like compound ER803022 (concentration 1 mg/ml) in buffer (A) and at equimolar content of Mg^{2+} (B). The top diagram (A) was adapted from Brandenburg et al [51].

Fig. 12: Temperature dependence of the peak position of the symmetric stretching vibration of the methylene groups (FTIR measurement)) for the hexaacyl phospholipid-like compound ER803022 in buffer and at equimolar content of Mg^{2+}.

Fig. 13: Small-angle X-ray diffraction pattern at 20 and 30 °C (A) and 35 and 50 °C, exhibiting in (A) a $L_\beta \leftrightarrow L_\alpha$ and in (B) a $L_\alpha \leftrightarrow H_{II}$ transition.

References

1. S. J. Singer, G. L. Nicolson, Science 173 (1972) 720-731.
2. H.-J. Gabius. S. Gabius, Glycosciences, status and perspectives, Chapman & Hall, London, 1997.
3. W. Curatolo, Biochim. Biophys. Acta 906 (1987) 137-160.
4. C. Langlet, A.-M. Bernard, P. Drevot, H.-T. He, Curr. Opin. Immunol. 12 (2000) 250-255.
5. M. Triantafilou, K. Miyake, D. T. Golenbock, K. Triantafilou, J. Cell Sci. 115 (1999) 2603-2611.
6. G. Cevc, Chem. Phys. Lipids 64 (1993) 163-186.
7. D. Chapman, D., C.J. Kirby, G. Gregoriadis, D.W. Deamer, D. R.L. Hamilton, L.S.S. Guo, P.I. Lelkes, N. Gains, H. Hauser, H.G. Weder, O. Zumbuehl, T.M. Allen, D.S. Johnston, J. Freise, A.W. T. Konings, P. Guiot, P. Baudhuin, E. Erikson, M.W. Fountain, G. Strauss, P. Machy, L.D. Leserman, S. Frokjær, E.L. Hjorth, O. Worts, L.S. Rao, Liposome Technology, Volume I, Preparation of Liposomes, CRC Press, Boca Raton, Florida, 1984.
8. C. Galanos, O. Lüderitz, O. Westphal, Eur. J. Biochem. 9 (1969) 245-249.
9. K. Brandenburg, M. H. J. Koch, U. Seydel, J. Struct. Biol. 105 (1990) 11-21.
10. L. D. Hawkins, S. T. Ishizaka, P. McGuinness, H. M. Zhang, W. Gavin, B. Decosta, Z. Y. Meng, H. Yang, M. Mullarkey, D. W. Young, D. P. Rossignol, A. Nault, J. Rose, M. Przetak, J. C. Chow, F. Gusovsky, J. Pharmacol. Exp. Ther. 300 (2002) 655-661.
11. R. Willumeit, M. Kumpugdee, S.S. Funari, K. Lohner, B. Pozo Navas, K. Brandenburg, S. Linser, J. Andrä, Biochem. Biophys. Acta 1669 (2005) 125-134.
12. G. Jürgens, M. Müller, P. Garidel, M. H. J. Koch, H. Nakakubo, A. Blume, K. Brandenburg, J. Endotoxin Res. 8 (2002) 115-126.
13. K. Brandenburg, G. Jürgens, J. Andrä, B. Lindner, M. H. J. Koch, A. Blume, P. Garidel, Eur. J. Biochem. 269 (2002) 5972-5981.

14. A. Blume, P. Garidel, in R. B. Kemp, (Ed.), From Macromolecules to Man, Elsevier, 1999, pp. 109-173.

15. M. H. J. Koch, J. Bordas, Nucl. Instr. Meth. 208 (1983) 461-469.

16. A. Gabriel, Rev. Sci. Instrum. 48 (1977) 1303-1305.

17. K. Brandenburg, W. Richter, M. H. J. Koch, H. W. Meyer, U. Seydel, Chem. Phys. Lipids 91 (1998) 53-69.

18. U. Seydel, H. Labischinski, M. Kastowsky, K. Brandenburg, Immunobiol. 187 (1993) 191-211.

19. U. Seydel, A. Wiese, A. B. Schromm, K. Brandenburg, in D. Morrison, H. Brade, S. Opal, S. Vogel, (Eds.), Endotoxin in Health and Disease, Marcel Dekker, New York, 1999, pp. 195-220.

20. A. Blume, Thermochim. Acta 193 (1991) 299-347.

21. J.N. Israelachvili, Intermolecular and surface forces, Academic Press, London, 1991.

22. M. K. Jain (1983) in R. C. Aloia, (Ed.), Membrane Fluidity in Biology, Vol. I: Concepts of Membrane Structure, Academic Press, 1983, pp. 1-37.

23. D. Dapman, Q. Rev. Biophys. 8 (1975) 185-235

24. R.L. Amey, D. Chapman, in D. Chapman (Ed.), Biomembrane Structure and Function, Verlag Chemie, Weinheim, 1984, pp. 199-256

25. N. Albon, J.M. Sturtevant, Proc. Natl. Acad. Sci. 75 (1978) 2258-2260

26. S.C. Chen, J.M. Sturtevant, B.J. Gaffney, Proc. Natl. Acad. Sci. 77 (1980) 5060-5063

27. R. Koynova, M. Caffrey, Biochim. Biophys. Acta 1376 (1998) 91-145

28. L. S. Lepore, J. F. Ellena, D. S. Cafiso, Biophys. J. 61 (1992) 767-775.

29. A. Mellier, Chem. Phys. Lipids 46 (1988) 51-56.

30. H. Träuble, Naturwissenschaften, 58 (1971) 277-284.

31. S. Mabrey and J. M. Sturtevant, Proc. Natl. Acad. Sci.73 (1978) 3862- 3866.

32. A. Blume, Biochemistry 22 (1983) 5436-5442.

33. A. Blume, Biochemistry 19 (1980) 4908-4913.

34. P. Privalov, N. N. Khechinashvili, J. Mol. Biol. 86 (1974) 665-684.

35. P. Garidel, W. Richter, G. Rapp, A. Blume, Phys. Chem. Chem. Phys. 3 (2001) 1504-1513.

36. P. Garidel, A. Blume, Langmuir 15 (1999) 5526-5534.

37. P. Garidel, A. Blume, Biochim. Biophys. Acta 1466 (2000) 245-259.

38. P. Garidel, G. Förster, W. Richter, B.H. Kunst, G. Rapp, A. Blume, Phys. Chem. Chem. Phys. 2 (2000) 4537-4544

39. A. Ferraretto, M. Pitto, P. Palestini, M. Masserini, Biochemistry 36 (1997) 9232-9236.

40. A. Terzaghi, G. Tettamanti, M. Masserini, Biochemistry 32 (1993) 9722-9725.

41. T. Harder, K. Simons, Curr. Opin. Cell Biol. 9 (1997) 534-542.

42. E. Th. Rietschel, T. Kirikae, F. U. Schade, U. Mamat, G. Schmidt, H. Loppnow, A. J. Ulmer, U. Zähringer, U. Seydel, F. Di Padova, M. Schreier, H. Brade, FASEB J. 8 (1994) 217-225.

43. M. Caffrey, J. Hogan, Chem. Phys. Lipids 61 (1992) 1-109.

44. K. Brandenburg, U. Seydel, Eur. J. Biochem. 191 (1990) 229-236.

45. P. Garidel, C. Johann, A. Blume, J. Therm. Anal. Calorimetry (2005), in press

46. P. Garidel, C. Johann, A. Blume. J. Liposome Res. 10 (2000) 131-158.

47. M. Rappolt, A. Kickel, F. Bringezu, K. Lohner, Biophys. J. 84 (2003) 3111-3122

48. K. Brandenburg, I. Moriyon, M. D. Arraiza, G. Lehwark-Yvetot, M. H. J. Koch, U. Seydel, Thermochim. Acta 382 (2002) 189-198.

49. H.H. Mantsch, R.N. McElhaney, Chem. Phys. Lipids 57 (1991) 13-26.

50. U. Seydel, L. Hawkins, A. B. Schromm, H. Heine, O. Scheel, M.H.J. Koch, K. Brandenburg, Eur. J. Immunol. 33 (2003) 1586-1592.

51. K. Brandenburg, L. Hawkins, P. Garidel, J. Andrä, M. Müller, H. Heine, M.H.J. Koch, U. Seydel, Biochemistry 43 (2004) 4039-4046.

52. A. Mellier, Chem. Phys. Lipids 51 (1989) 23-29.

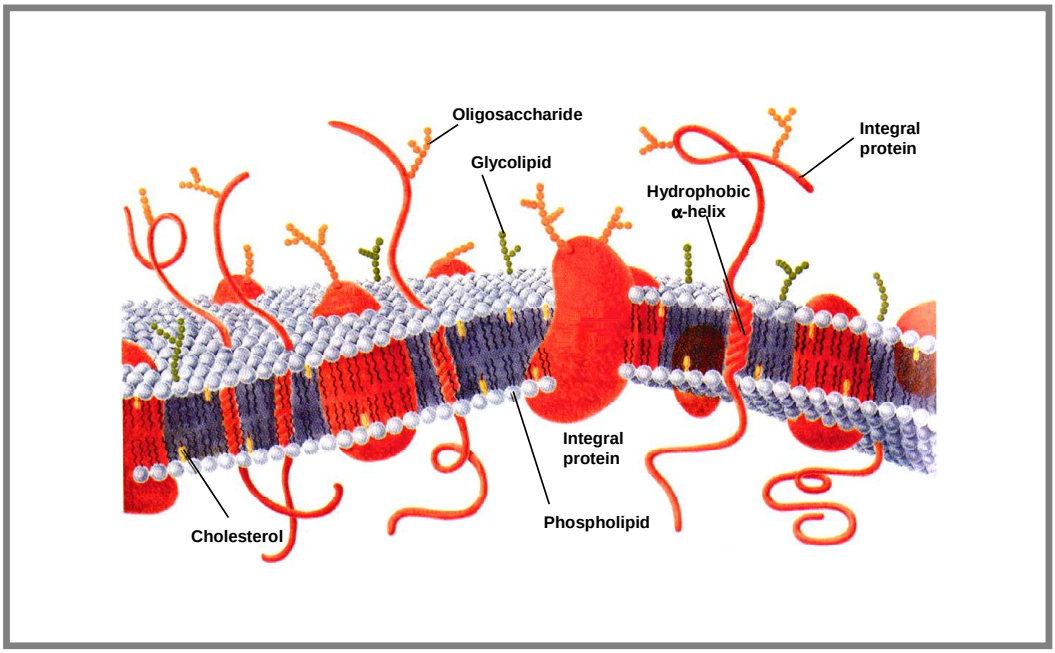
Oligosaccharide
Glycolipid
Integral protein
Hydrophobic α-helix
Integral protein
Phospholipid
Cholesterol

Fig. 1

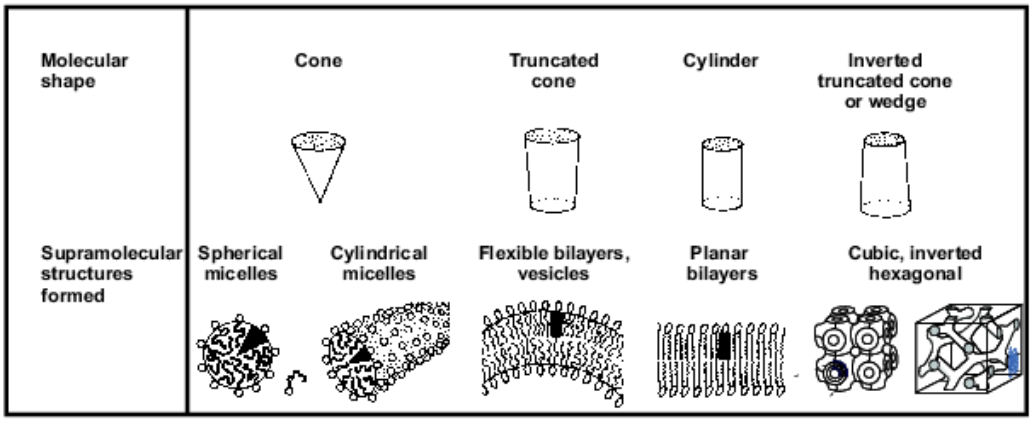
Molecular shape
Cone
Truncated cone
Cylinder
Inverted truncated cone or wedge
Supramolecular structures formed
Spherical micelles
Cylindrical micelles
Flexible bilayers, vesicles
Planar bilayers
Cubic, inverted hexagonal

Fig. 2

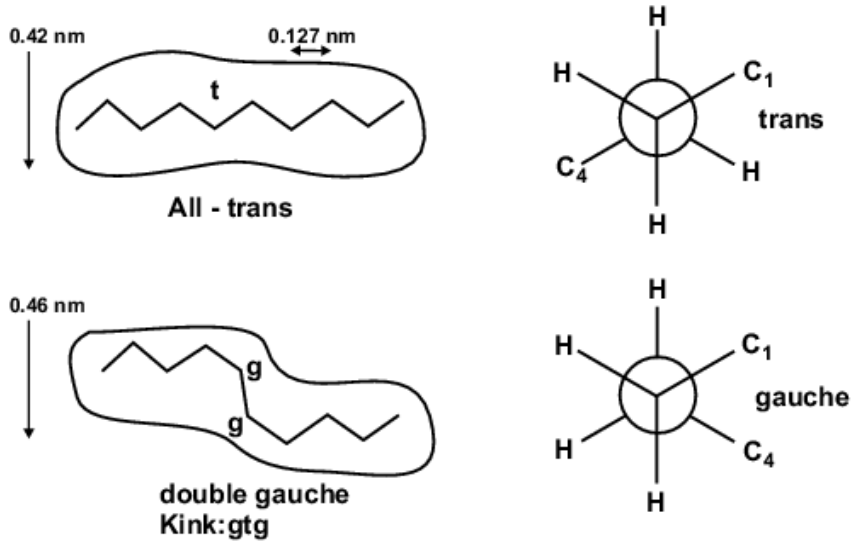
0.42 nm
0.127 nm
t
All - trans
H
H
C1
trans
C4
H
H
0.46 nm
g
g
double gauche
Kink:gtg
H
H
C1
gauche
H
C4
H

Fig. 3

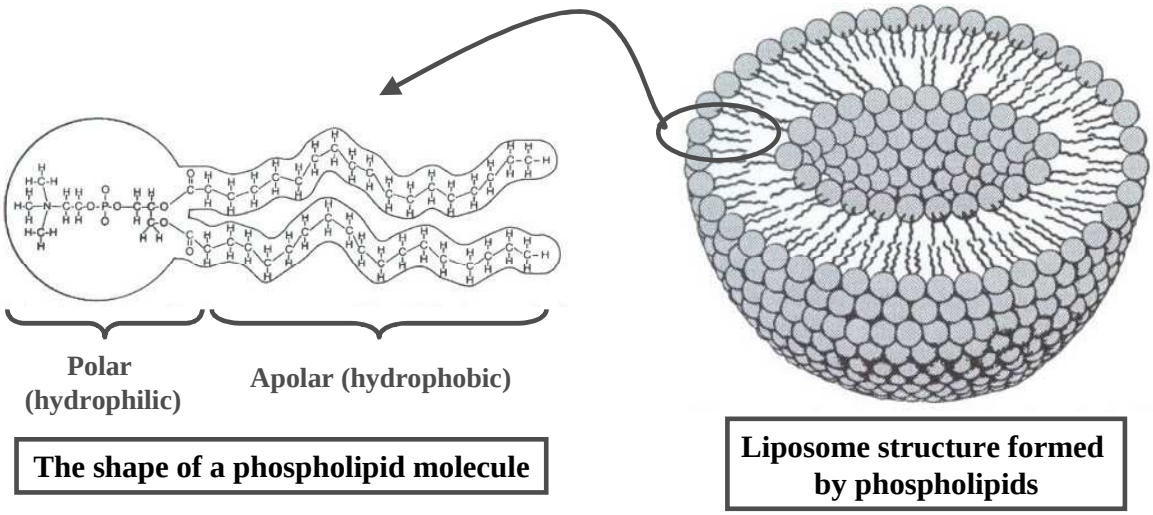
Polar
(hydrophilic)
Apolar (hydrophobic)
The shape of a phospholipid molecule
Liposome structure formed by phospholipids

Fig. 4

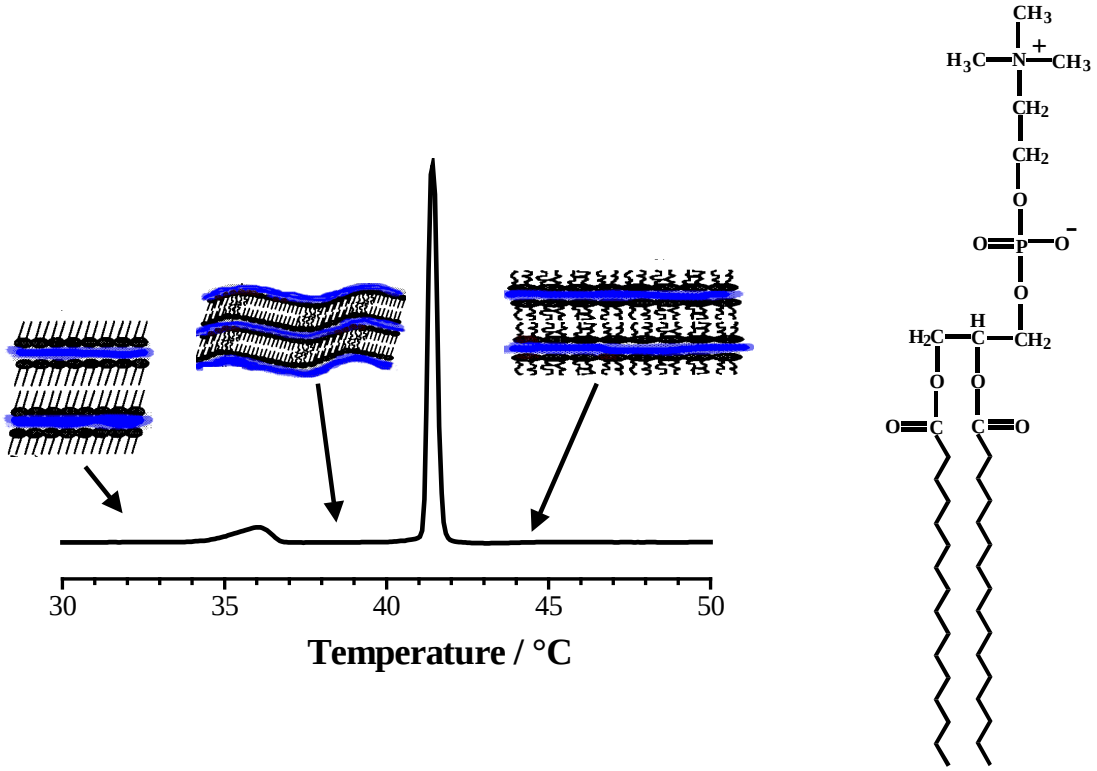

Fig. 5

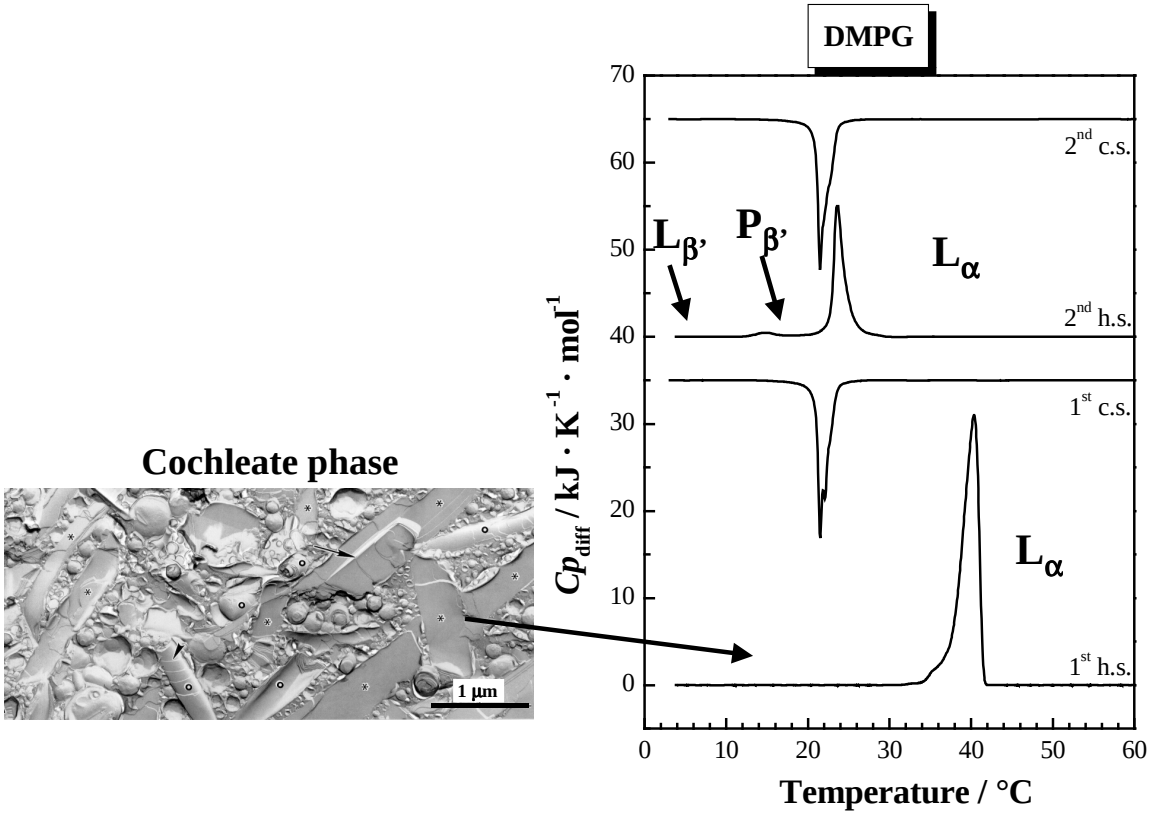
DMPG
Cochleate phase
1 µm
$L_{\beta'}$
$P_{\beta'}$
L_α
L_α
2nd c.s.
2nd h.s.
1st c.s.
1st h.s.
Cp_{diff} / kJ · K^{-1} · mol^{-1}
Temperature / °C
0
10
20
30
40
50
60
70

Fig. 6

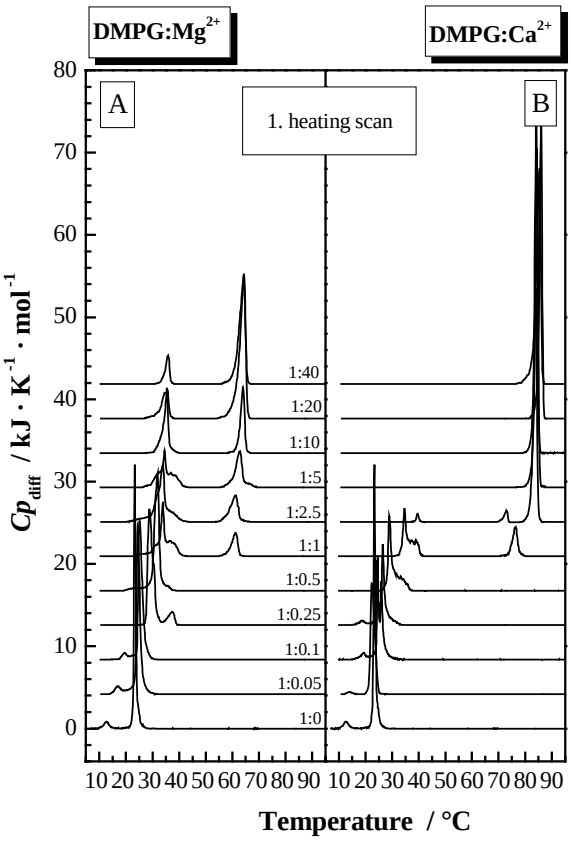
DMPG:Mg2+
DMPG:Ca2+
A
B
1. heating scan
1:40
1:20
1:10
1:5
1:2.5
1:1
1:0.5
1:0.25
1:0.1
1:0.05
1:0
Cp_diff / kJ · K-1 · mol-1
Temperature / °C

Fig. 7

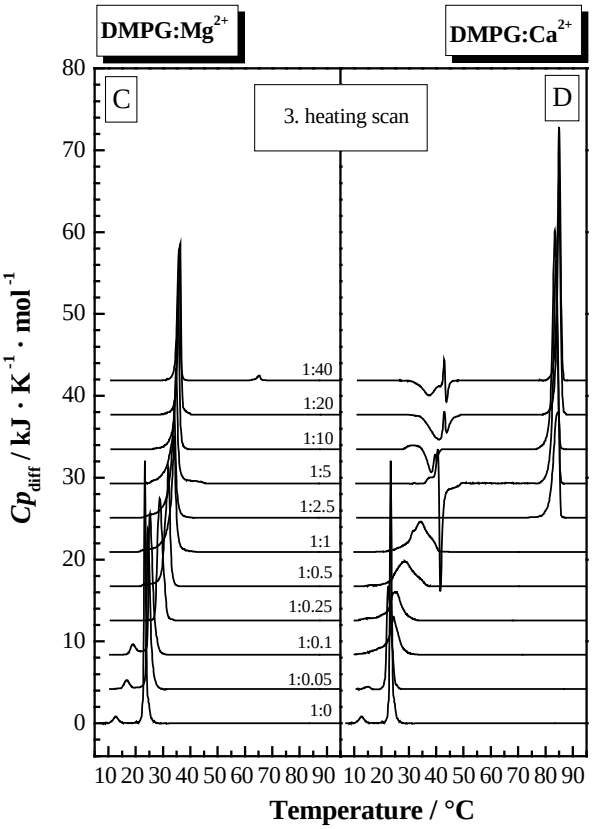
DMPG:Mg2+
DMPG:Ca2+
C
D
3. heating scan
1:40
1:20
1:10
1:5
1:2.5
1:1
1:0.5
1:0.25
1:0.1
1:0.05
1:0
Cp_diff / kJ · K-1 · mol-1
Temperature / °C
0 10 20 30 40 50 60 70 80
10 20 30 40 50 60 70 80 90

Fig.7

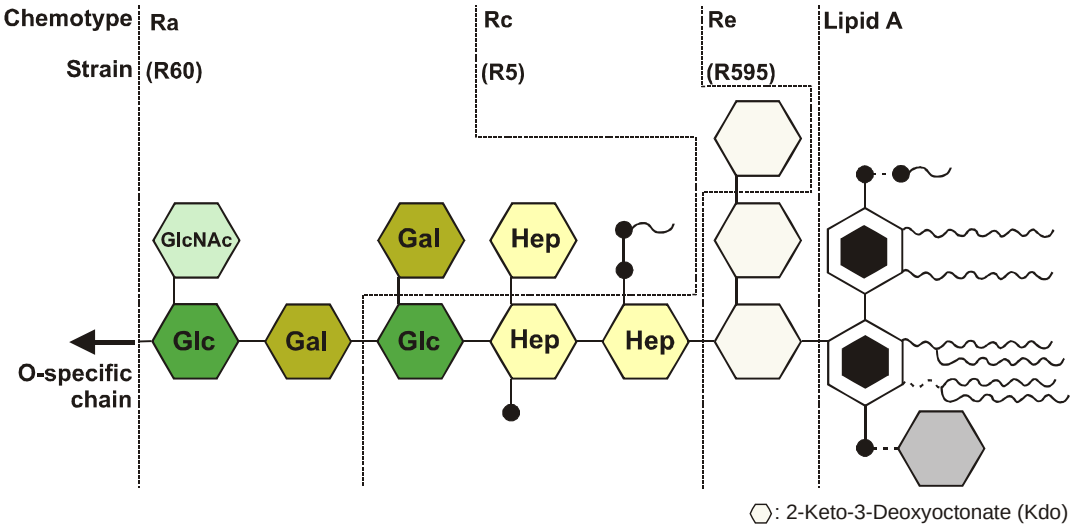
Chemotype
Strain
Ra
(R60)
Rc
(R5)
Re
(R595)
Lipid A
GlcNAc
Gal
Hep
Glc
Gal
Glc
Hep
Hep
O-specific chain
⎔: 2-Keto-3-Deoxyoctonate (Kdo)

^

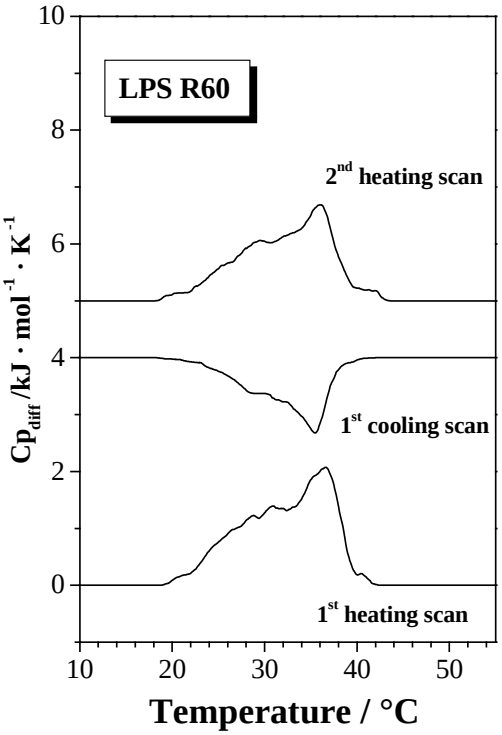
LPS R60
2nd heating scan
1st cooling scan
1st heating scan
Cpdiff /kJ · mol-1 · K-1
Temperature / °C
10
8
6
4
2
0
10
20
30
40
50

Fig. 8

Figure 7

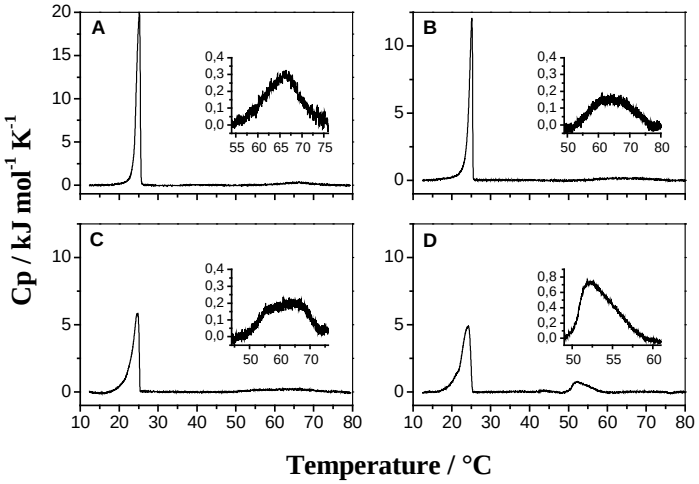

Fig. 9

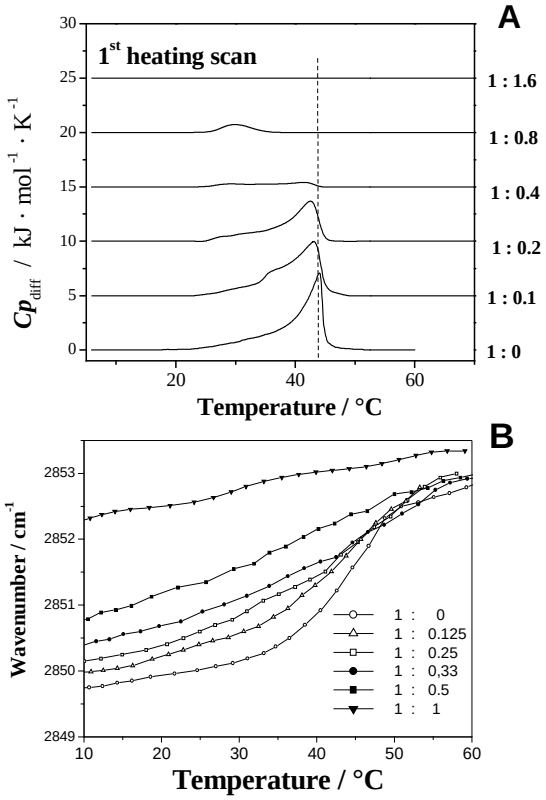
A
1st heating scan
1 : 1.6
1 : 0.8
1 : 0.4
1 : 0.2
1 : 0.1
1 : 0
Cp_diff / kJ · mol-1 · K-1
Temperature / °C
B
Wavenumber / cm-1
1 : 0
1 : 0.125
1 : 0.25
1 : 0,33
1 : 0.5
1 : 1
Temperature / °C

Fig. 10

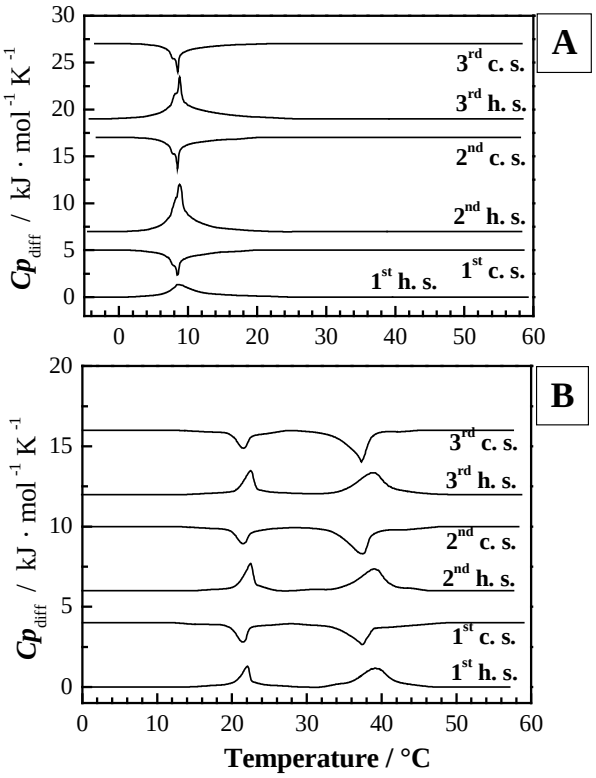
A
B
3rd c. s.
3rd h. s.
2nd c. s.
2nd h. s.
1st c. s.
1st h. s.
Cp diff / kJ · mol -1 K -1
Temperature / °C
0
5
10
15
20
25
30
0
10
20
30
40
50
60

Fig. 11

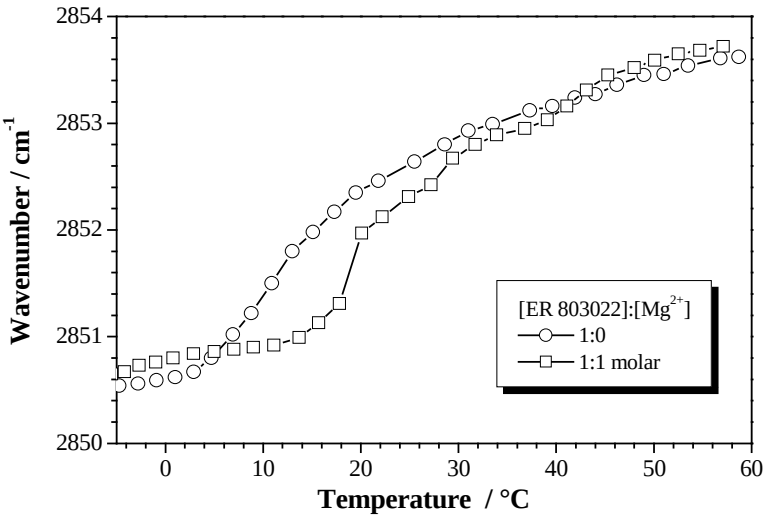
2854
2853
2852
2851
2850
Wavenumber / cm-1
0
10
20
30
40
50
60
Temperature / °C
[ER 803022]:[Mg2+]
1:0
1:1 molar

Fig 12

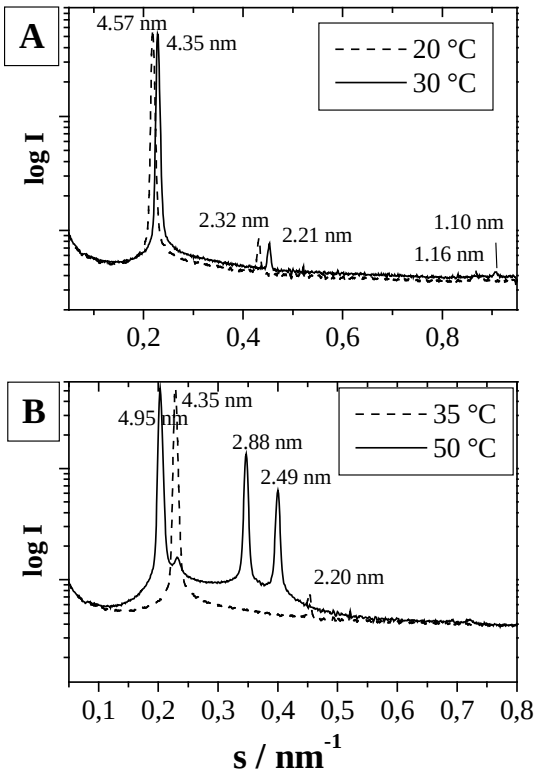
A
4.57 nm
4.35 nm
20 °C
30 °C
log I
2.32 nm
2.21 nm
1.10 nm
1.16 nm
0,2
0,4
0,6
0,8
B
4.35 nm
4.95 nm
35 °C
50 °C
2.88 nm
2.49 nm
log I
2.20 nm
0,1
0,2
0,3
0,4
0,5
0,6
0,7
0,8
s / nm-1

Fig. 13